Comparing the cyclic behavior of concrete cylinders confined by shape memory alloy wire or steel jackets

2011 Smart Mater. Struct. 20 094008

(http://iopscience.iop.org/0964-1726/20/9/094008)

Smart Mater. Struct. **20** (2011) 094008 (11pp) doi:10.1088/0964-1726/20/9/094008

Comparing the cyclic behavior of concrete cylinders confined by shape memory alloy wire or steel jackets

Joonam Park[1], **Eunsoo Choi**[2], **Kyoungsoo Park**[3,4] **and Hong-Taek Kim**[2]

[1] Department of Civil and Environmental Engineering, WonKwang University, Iksan 570-749, Korea
[2] Department of Civil Engineering, Hongik University, Seoul 121-791, Korea
[3] School of Civil and Environmental Engineering, Yonsei University, Seoul 120-749, Korea

E-mail: joonam.park@gmail.com, eunsoochoi@hongik.ac.kr, k-park@yonsei.ac.kr and htaek@hongik.ac.kr

Received 20 November 2010, in final form 25 June 2011
Published 30 August 2011
Online at stacks.iop.org/SMS/20/094008

Abstract
Shape memory alloy (SMA) wire jackets for concrete are distinct from conventional jackets of steel or fiber reinforced polymer (FRP) since they provide active confinement which can be easily achieved due to the shape memory effect of SMAs. This study uses NiTiNb SMA wires of 1.0 mm diameter to confine concrete cylinders with the dimensions of 300 mm × 150 mm ($L \times D$). The NiTiNb SMAs have a relatively wider temperature hysteresis than NiTi SMAs; thus, they are more suitable for the severe temperature-variation environments to which civil structures are exposed. Steel jackets of passive confinement are also prepared in order to compare the cyclic behavior of actively and passively confined concrete cylinders. For this purpose, monotonic and cyclic compressive loading tests are conducted to obtain axial and circumferential strain. Both strains are used to estimate the volumetric strains of concrete cylinders. Plastic strains from cyclic behavior are also estimated. For the cylinders jacketed by NiTiNb SMA wires, the monotonic axial behavior differs from the envelope of cyclic behavior. The plastic strains of the actively confined concrete show a similar trend to those of passive confinement. This study proposed plastic strain models for concrete confined by SMA wire or steel jackets. For the volumetric strain, the active jackets of NiTiNb SMA wires provide more energy dissipation than the passive jacket of steel.

(Some figures in this article are in colour only in the electronic version)

1. Introduction

Shape memory alloys (SMAs) are rising as a smart material, and their applications for civil structures are increasing because they show particular advantages such as superelasticity and the shape memory effect which are desirable for seismic retrofits as well as new construction of reinforced concrete (RC) structures. Superelastic SMA bars have been used for RC columns in new construction to improve seismic performance [1, 2]. The studies embedded superelastic SMA bars for longitudinal reinforcement to replace steel reinforcements in the plastic hinge region in order to increase the recentering capacity and, thus, reduce the residual displacement in RC columns. SMA wire jackets were applied to confine the concrete and to retrofit RC columns that do not show satisfactory seismic performance [3–5]. In the applications, the developed recovery stress due to the shape memory effect provided active confining pressure on the concrete, and the SMA wire jackets increased the peak strength of the concrete and the displacement ductility of the RC columns; this was critical for improving the seismic performance of RC columns. Superelastic SMA bars were used to improve the moment-rotation behavior at beam–column joints. Youssef *et al* [6] placed SMA bars at the beam–

[4] Author to whom any correspondence should be addressed.

column joint of a RC frame instead of steel reinforcement. They also provided a coupling method between the SMA bar and steel reinforcing bar. The employment of superelastic SMA bars relocated the plastic hinge region away from the column face. SMA bars were also applied for steel beam–column joints [7]. In the study, martensitic SMA tendons were used, and they absorbed a large rotational energy and protected the yield of beams and columns. Penar [8] introduced superelastic SMA bars as the load transferring medium at steel beam–column joints. The exploitation of superelastic SMA bars improved a recentering moment-rotational behavior. The seismic performance of both connections of martensitic and superelastic SMA tendons for steel beam–column joints were analytically estimated and indicated that superelastic SMA connections were most effective in restraining residual deformation demands [9]. Hu *et al* [10] investigated the performance of composite-moment frames with concrete-filled tube columns with superelastic SMA tendons analytically and provided numerical modeling methods.

DesRoches *et al* [11] conducted cyclic tensile tests of superelastic SMA wires and bars to evaluate the mechanical properties under cyclic loading. DesRoches and his colleagues tried to evaluate the seismic application of the superelastic bars as a seismic restrainer for multiple span simply supported or multiple frame bridges [12–14]. The SMA bar restrainers were effective for reducing the relative displacement at internal hinges and, thus, effective for preventing the unseating of bridge decks. They also compared between SMA restrainers and other bridge retrofit devices and interpreted the effect of tension only and tension/compression SMA restrainers. Choi *et al* [15] conducted reversed cyclic bending tests of superelastic SMA bars and investigated the mechanical properties of the bending SMA bars. They also introduced the bending SMA bar as a bridge restrainer and compared its seismic performance to prevent unseating of bridges with other types of restrainers [16]. They indicated that the tension/compression SMA restrainer can be exposed to a buckling problem as indicated by Wilde [17], however, the bending SMA restrainer was free from the buckling and, thus, the bending SMA restrainers would be practical to install in real bridges.

The shape memory effect and the superelastic behavior of SMA wires or bars are often exposed to cyclic conditions, and the mechanical properties of SMAs vary under cyclic loadings. In order to obtain stable mechanic behavior of SMAs, mechanical training has been proposed to limit degradation of the functions and fatigue life [18]. McCormick *et al* [19] investigated the effect of mechanical training on the properties of superelastic SMAs for seismic applications according to the number of training cycles, the strain level, and the loading rate. Kim and Cho [20] used the thermal trained SMA wires to develop a smart wing actuator. The thermal training applied cyclic loadings under temperature variation and provided repeated hysteretic curves due to the saturation of permanent deformation.

The shape memory effect of SMAs was proved to be effective to confine concrete and increase the peak strength and ductility of concrete [3, 5]. Both studies investigated the recovery and the residual stresses developed due to the shape memory effect. These studies demonstrated that SMA wire or ring jackets provided active confinement of concrete. Also, they used an NiTiNb SMA that showed wider temperature hysteresis than the general NiTi SMAs. Choi *et al* [3] explained the benefit of a wide temperature hysteresis when the shape memory effect is applied for civil structures. For the application of the shape memory effect of SMAs, the martensitic SMA wires or rings should be prestrained and can be stored under air temperature where the SMAs are exposed to. The A_s temperature should be higher than the highest air temperature in the region and, thus, the deformed SMA wires or rings can be stored without recovering the prestrain. Also, the residual stress should be retained under the lowest air temperature; therefore, the M_s temperature should be lower than the lowest air temperature in the region. The NiTiNb SMAs are suitable to satisfy the above condition, and they show a relatively wide temperature hysteresis when they are prestrained.

Table 1. Temperature widows of the NiTiNb SMA wires according to prestrain.

Prestrain	M_s (°C)	M_f (°C)	A_s (°C)	A_f (°C)	As–M_s (°C)
Without prestrain	−33.7	−65.9	−9.5	22.0	24.2
With prestrain	−17.6	−74.3	104.9	139.2	122.5

This study used NiTiNb SMA wire jackets and steel jackets to confine concrete cylinders. The SMA wire jackets provide active and passive confinement, although the steel jackets provide only passive confinement. The goals of this study are to assess the cyclic axial behavior of concrete cylinders confined by the active SMA wire and the passive steel jackets and to compare them.

2. SMA wires and steel plates

This study used SMA wire of $Ni_{47.4}$–$Ti_{37.86}$–$Nb_{14.69}$ (wt. %) with the diameter of 1.0 mm. The alloy was manufactured by high-frequency vacuum-induction melting and then hot-rolled into wires with a diameter of 1.075 mm at 850 °C. The hot-rolled wires were reduced the diameter into 1.0 mm by cold drawing without intermediate annealing. During the process, some amount of prestrain in axial direction was introduced into the wire. Table 1 shows the temperature windows of the wires without prestrain and with the prestrain. The temperature window of the wire without prestrain was not suitable for civil applications because the A_s was too low to store deformed SMA wires under general air temperature in regions with high seismic activity, such as the United States, Japan, and New Zealand. However, the window of the prestrained wire matched the required temperature. The temperature hysteresis of A_s–M_s increased by 98.3 °C due to the prestrain.

The recovery and the residual stress of the SMA wires were measured by varying the level of prestrain from 1% to 7%. The wires were heated up to 200 °C to produce recovery stress and cooled down to room temperature (approximately

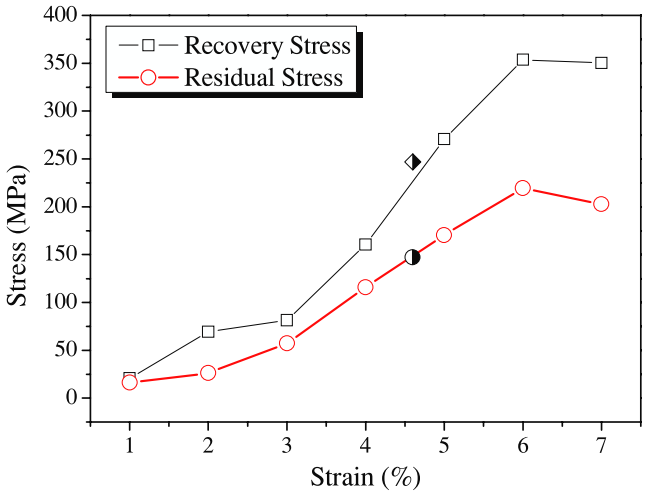

Figure 1. Recovery and residual stress as a function of prestrain.

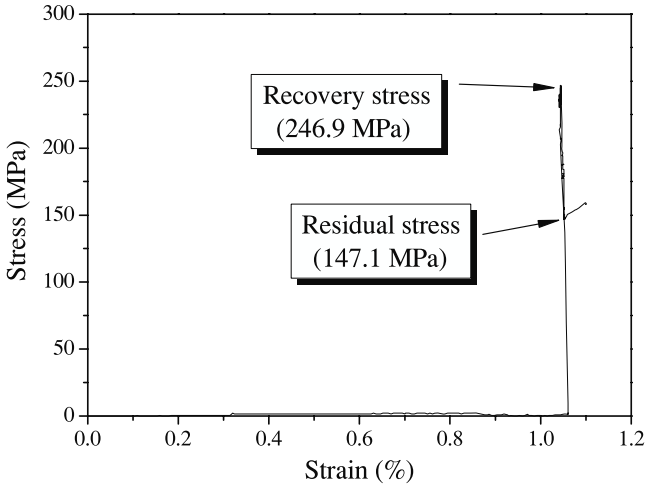

Figure 2. Recovery and residual stress of the manufactured SMA wire.

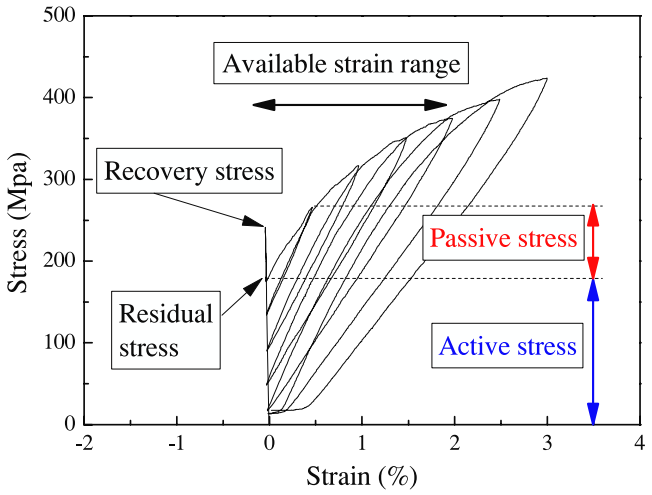

Figure 3. Hysteretic behavior of the SMA wire under residual stress.

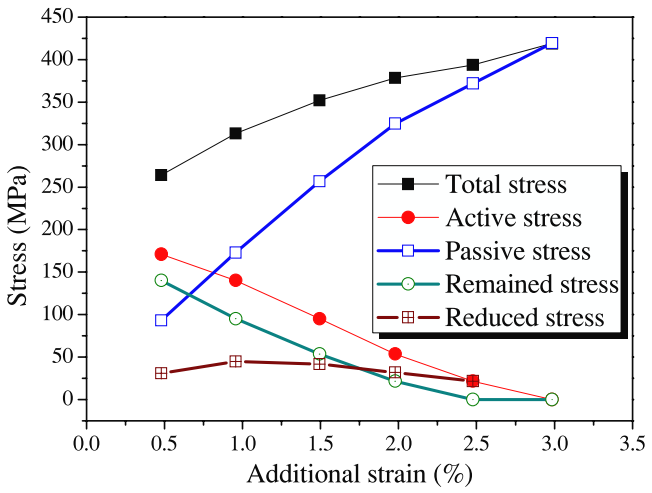

Figure 4. Variation of active and passive stress due to additional strain.

15 °C). The recovery stress was reduced to the residual stress by cooling the wire temperature since the recovery stress depends on temperature even though state transformation does not occur. As shown in figure 1, the maximum recovery and residual stress were developed at 6% prestrain, and the corresponding values were 353.7 MPa and 219.5 MPa, respectively. Figure 2 shows the process of measuring the prestrained wire during the manufacturing process. The recovery and the residual stress of the prestrained wire were 246.9 MPa and 147.1 MPa, respectively. Comparing these values to those in figure 1, the prestrain was estimated to be 4.6%. Stainless steel plates of 1.0 and 1.5 mm thickness were used in this study, and their yield strength was measured to be 250 MPa.

3. Behavior of SMA wire under residual stress

Choi *et al* [4] explained the tensile behavior of the martensitic SMA wires under residual stress. They indicated that the loading path from the residual stress passed through the unloading point in the stress–strain curve of the SMA wire; they found this using insight during the measurement of the recovery and residual stress of SMA wires. Also, they mentioned that the available strain range was the same as the recovered strain. When the applied strain exceeds the available strain range, the residual strain remained. This study measured the tensile behavior of the NiTiNb SMA wire under residual stress to prove experimentally the above detection. In figure 3, the prestrained wire was heated up to 200 °C and cooled down. During this process, the measured recovery and the residual stress were 241.0 MPa and 171.0 MPa, respectively. This corresponded to the measured stresses in figure 2 almost perfectly. Additional strains were applied under residual stress that acted as active confinement. Generally, the remaining residual stress decreased with increasing additional strain. Also, the available strain range was estimated to be 2.2%. Figure 4 shows the variation of active and passive stress with the applied additional strain. In the figure, the total stress was the summation of the active and passive stress. The active

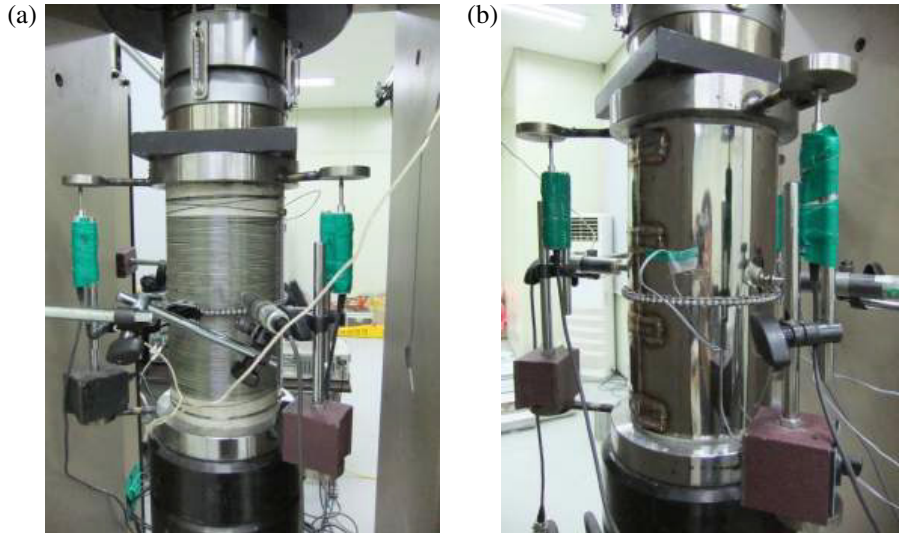

Figure 5. Test setup for compressive tests. (a) SMA wire jacket. (b) Steel jacket.

stress was the remaining residual stress that provided active confinement when the additional strain began. The passive stress developed due to the additional strain, and the remaining stress was measured when the unloading was completed to the original strain. Thus, the previous remaining stress acted as the active stress for the next additional strain procedure. The final reduced stress was the amount of stress reduction due to a loading and unloading cycle. Thus, the summation of the remaining stress and the reduced stress was equal to the active stress. The active stress and the remaining stress decreased with increasing additional strain. When the additional strain reached 2.48%, the remaining stress became zero because the applied strain exceeded the available strain range of 2.2%. The total stress increased with increasing additional strain because the passive stress increased. The reduced stress was almost constant with variation of the additional strain and thus, it seems that the reduced stress is a characteristics of the NiTiNb SMA wire.

At first, the wire strained with the active stress of 171 MPa and reached 0.48% strain where the total stress was 264 MPa. The passive stress was 93 MPa. Then, the wire was unloaded to the original location, and the remaining stress was 140 MPa. During the cycle, the reduced stress was 31 MPa. For the next step, the remaining stress of 140 MPa acted as the active stress. As seen in figure 3, the active confinement for monotonic loading was constant, but it varied for the cyclic loading process.

4. Specimens and test setup

This study used concrete cylinders with a diameter of 150 mm and a length of 300 mm to obtain the cyclic compressive behavior of confined concrete, as shown in figure 5. The average peak strength of plain concrete was 36.4 MPa. SMA wire was wrapped around a concrete cylinder. It was then heated to over the temperature A_f following wrapping onto the concrete. Then, the recovery stress was developed and reduced to the residual stress by cooling. The residual stress provided active confinement. The SMA wire jacketing process was explained in detail in a previous study [21]. The center-to-center pitch of the wires was either 1.0 or 2.0 mm. A total of four specimens were prepared with SMA wire jackets; two were used for monotonic tests and the other two were used for cyclic tests.

For the steel jackets, 1.0 and 1.5 mm steel plates were used. The steel jacketing process was described in detail in the previous study [22]. The steel jacketing method differed from that of conventional steel jackets in that the method did not use grouting between the steel and concrete. The steel plates were pressed externally by clamps and welded at the overlapped line. Four steel-jacketed specimens were prepared for each thickness; one was used for the monotonic test and the other three were used for the cyclic tests. Three unjacketed cylinders were tested for reference. Figure 5 shows the setup for compressive tests. The axial deformation was measured by three displacement transducers located between sole plates located at the top and the bottom of specimens. Also, the circumferential dilation was measured by an extensometer located in the middle of each specimen. Each deformation in axial and circumferential direction was used to calculate the related strain. The loading speeds were 0.5 mm min^{-1} for the plain concrete and 1.0 mm min^{-1} for the jacketed specimens, respectively.

5. Test results I: axial direction

5.1. Axial behavior

The monotonic behavior of the specimens in the axial direction is shown in figure 6. The monotonic curves for the specimen confined by the SMA wire jackets with 1.0 mm pitch showed strength hardening following strength degradation after the peak strength; this differed from the curve of the steel-jacketed specimen. The strain in the SMA wire increased with

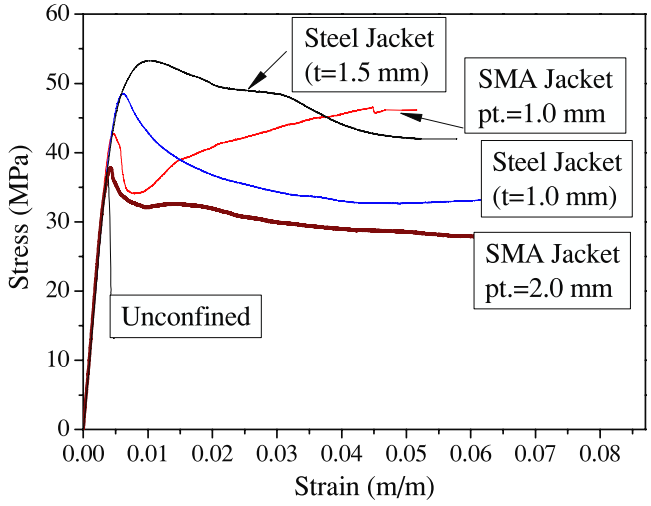

Figure 6. Monotonic behavior of unconfined and confined specimens.

increasing axial loading due to the bulge in the circumferential direction; thus, the developed stress in the wire increased as shown in figure 3. This increased stress seemed to produce the hardening behavior; however, the hardening was not clear for the specimen with 2.0 mm pitch because the lateral confinement introduced by the SMA wire was relatively small.

Figure 7 shows the cyclic behavior of the jacketed specimens. For the cyclic behavior, the envelopes of the hysteretic curves for the steel-jacketed specimens were close to those of the monotonic curves. However, the envelopes for the specimens confined by SMA wire jackets did not show hardening behavior and, thus, differed from the monotonic behavior. The cyclic loading and unloading reduced the active stress in the SMA wire as shown in figure 3; thus, hardening seemed not to be observed in the hysteretic behavior.

5.2. Plastic strains

The plastic strain of concrete is defined as the remaining strain in the axial direction when it is unloaded to zero stress. Previous studies have indicated that the plastic strain of unconfined or confined concrete was related to the axial strain at the envelope strain of unloading [23, 24]. Sakai and Kawashima [23] mentioned that the plastic strain ε_{pl} of confined concrete depended on the unloading strain ε_{un} linearly for the two regions of $0.001 < \varepsilon_{un} < 0.0035$ and $\varepsilon_{un} \geqslant$

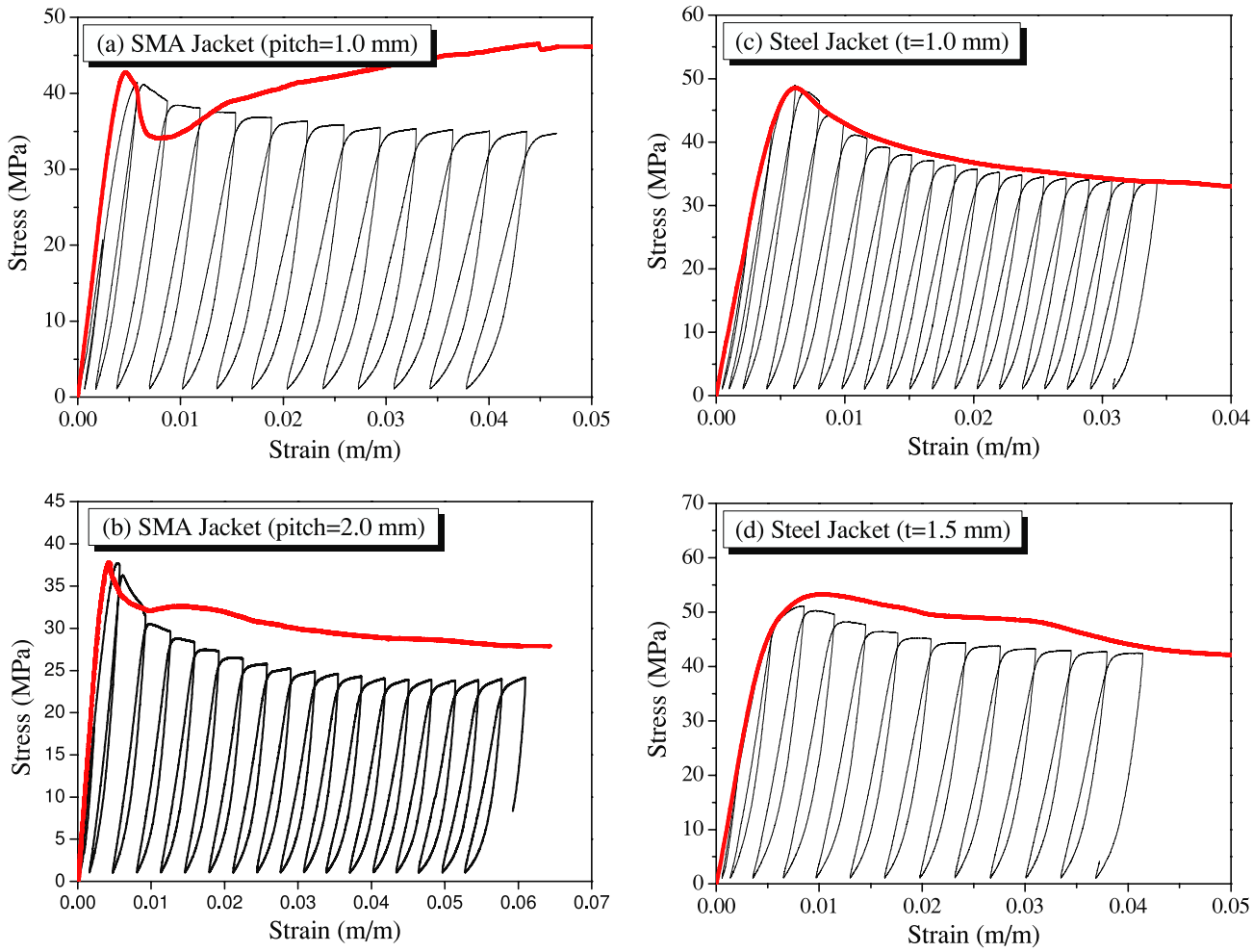

Figure 7. Cyclic behavior of confined specimens in axial direction. (a) SMA jacket with 1.0 mm pitch. (b) SMA jacket with 2.0 mm pitch. (c) Steel jacket with 1.0 mm thick. (c) Steel jacket with 1.5 mm thick.

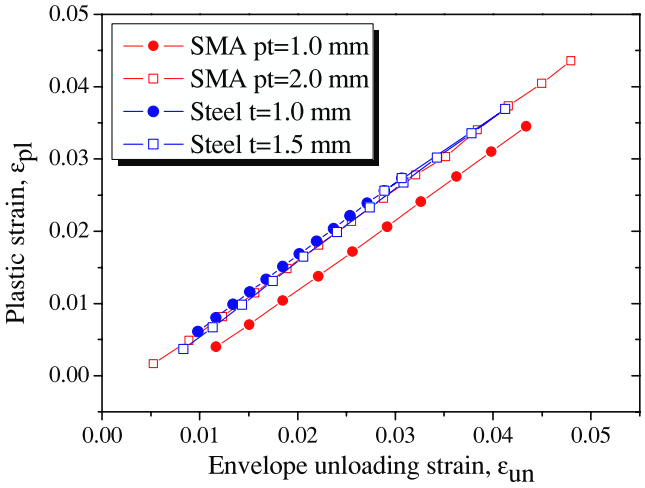

Figure 8. Plastic strains versus envelope unloading strains.

Table 2. Regressions for plastic strains of confined specimens.

Specimen	Slope	y-intercept	R^2
SMA-P1	0.924	−0.0061	0.9966
SMA-P2	0.985	−0.0039	0.9997
ST-10-1	1.027	−0.0040	0.9999
ST-10-2	1.008	−0.0050	0.9999
ST-10-3	1.007	−0.0047	0.9999
ST-15-1	1.013	−0.0046	0.9998
ST-15-2	1.004	−0.0057	1.0
ST-15-3	1.002	−0.0045	0.9997

0.0035. This study discussed the second region for confined concrete. Figure 8 shows the plastic strains of confined specimens as a function of the envelope unloading strain, and table 2 shows the slope, the y-axis intercept, and the R^2 for the regressions. The slopes for SMA wire jackets were 0.924 and 0.985 for the wires with 1.0 mm pitch and 2.0 mm pitch, respectively. Also, the average values were 1.014 and 1.006 for steel jackets of 1.0 and 1.5 mm thickness. Thus, the slope of the relationship between ε_{pl} and ε_{un} was almost the same for a material not related to the amount of confinement. Lam *et al* [25] estimated the slope for carbon fiber reinforced polymer (CFRP)-jacketed specimens to be 0.71. Consequently, the trend of the plastic strain for specimens confined by SMA wire jackets was similar to those confined by steel jackets but different from those confined by CFRP jackets.

Lam *et al* [25] proposed a model of plastic strain as a function of peak strength of plain concrete f'_{co} and unloading strain of envelopes ε_{un} which can be written as

$$\varepsilon_{pl} = (0.87 - 0.004 f'_{co})\varepsilon_{un} - 0.0016$$
$$0.0035 \leqslant \varepsilon_{un} \leqslant \varepsilon_{cu}. \quad (1)$$

where ε_{cu} represents the ultimate strain of concrete.

This equation was suggested for CFRP-jacketed concrete; therefore, this study modified the equation for SMA wire and steel jackets. The factor of −0.004 for the contribution of peak strength to the plastic strains is assumed to be equal for the SMA wire and steel jackets. Then, equation (1) can be

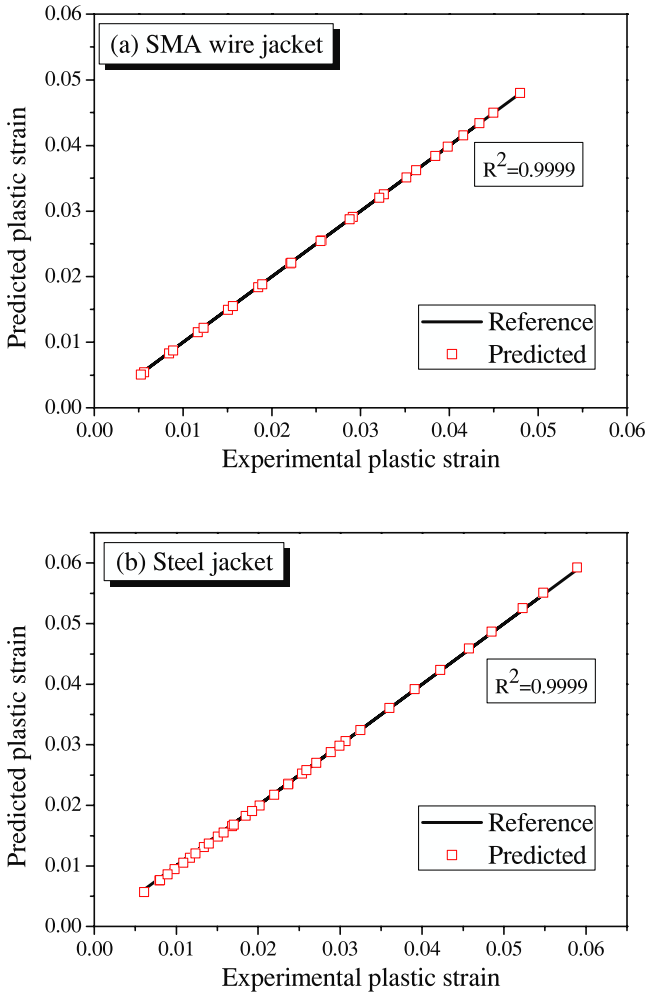

Figure 9. Plastic strain models for confined specimens. (a) SMA wire jacket. (b) Steel jacket.

Table 3. Constants for plastic strain model.

Jacket	α	β
SMA	1.15	0.0004
Steel	1.16	0.0005

modified as

$$\varepsilon_{pl} = (\alpha - 0.004 f'_{co})\varepsilon_{un} - \beta, \quad (2)$$

where α and β are constants to control the slope and the y-axis intersection of the equation. By a trial and error method, the constants were determined for the SMA wire and steel jackets as shown in table 3. The two equations for the plastic strains in table 3 are close to each other: thus, the concrete confined by the SMA wire and steel jackets produce almost the same plastic strains for unloading from the envelope curve. Figure 9 compares the predicted and experimental plastic strains. The performance of the suggested equations is almost perfect to reproduce experimental data.

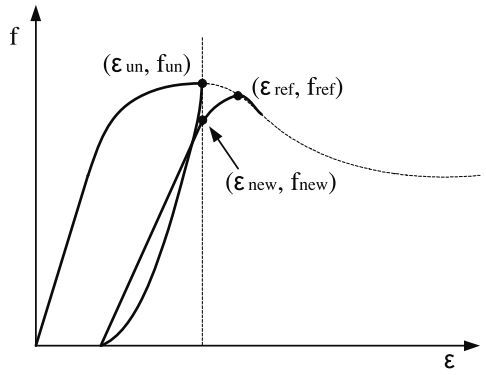

Figure 10. Schematic drawing for new and reference stress.

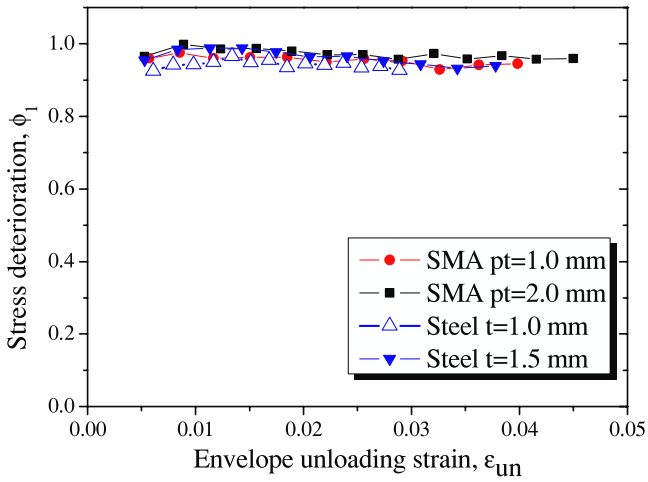

Figure 11. Stress deterioration ratio of confined specimens.

5.3. Stress deterioration

The new stress f_{new} is the stress point at the envelope unloading strain, and the reference stress f_{ref} is the stress where a reloading path meets the envelope curve again. The two stresses are explained in figure 10. The ratio of the new stress to the reference stress is called the stress deterioration ratio ϕ [23]. A general equation for the ratio is expressed by

$$\phi_n = \frac{f_{new,n}}{f_{ref,n}} \qquad (n = 1, 2, 3, \ldots) \tag{3}$$

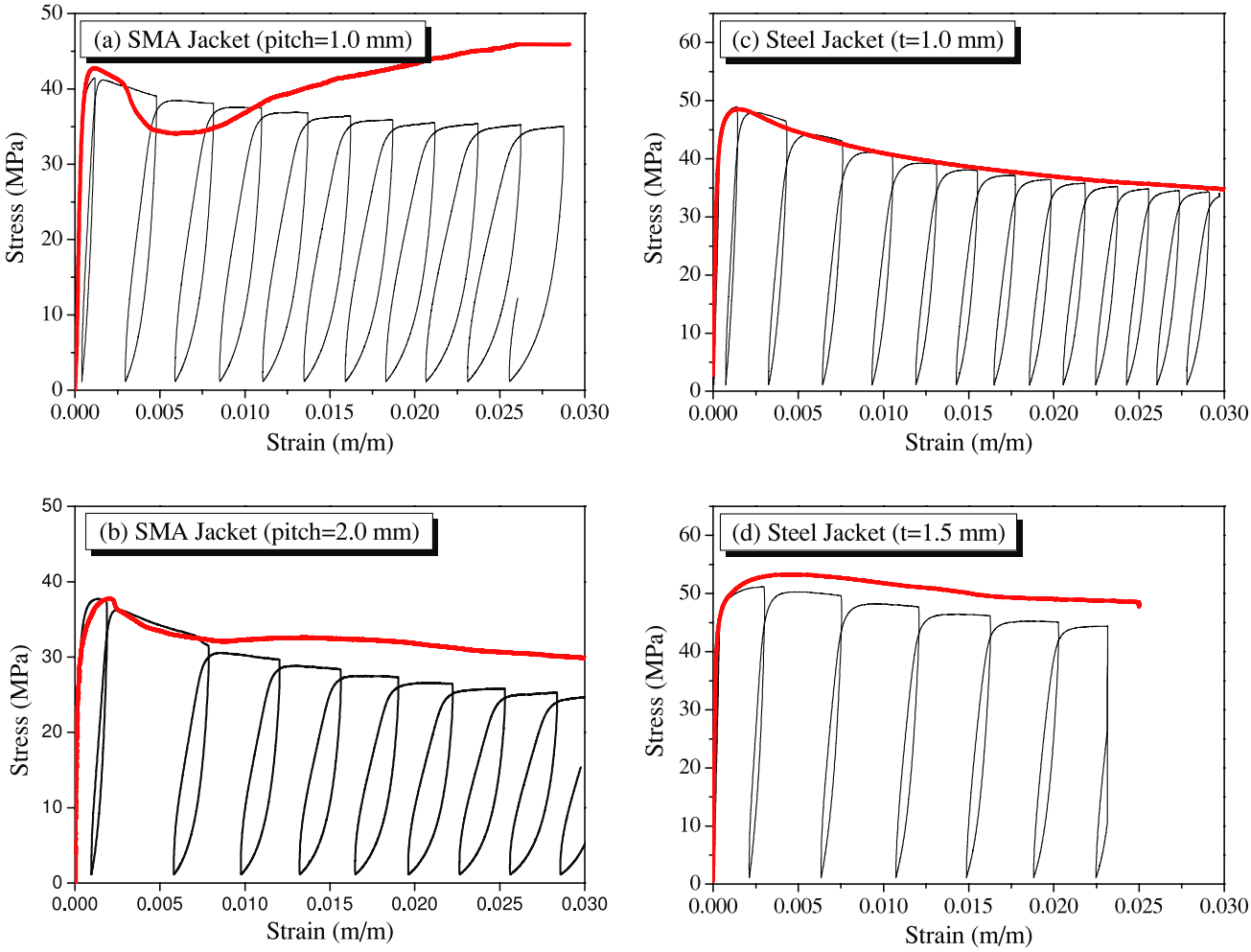

Figure 12. Cyclic behavior of confined specimens in circumferential direction. (a) SMA jacket with 1.0 mm pitch. (b) SMA jacket with 2.0 mm pitch. (c) Steel jacket with 1.0 mm thick. (d) Steel jacket with 1.5 mm thick.

where ϕ_n is the stress deterioration ratio for the nth unloading/reloading cycle; $f_{\text{new},n}$ and $f_{\text{ref},n}$ are the new stress and the reference stress for the nth reloading path. This study conducted only one cycle; thus, the ϕ_1 was estimated. Sakai and Kawashima [23] suggested the ratio of 0.92 for concrete confined by steel reinforcements when the unloading strain was larger than 0.0035. Also, Lam and Teng [25] used the same value for the FRP-jacketed concrete. Figure 11 shows the variation of the ratios with the variation of the envelope unloading strain. The average values were 0.96 and 0.97 for the SMA wire jackets with 1.0 mm and 2.0 mm pitch, respectively, and the value for the steel jackets was 0.94.

The SMA wire confined concrete showed a slightly larger ratio than that of the steel-jacket-confined concrete. However, the number of specimens for the SMA wire cases was very small since not enough wire was prepared. Therefore, more experimental tests are required to confirm the observations of this study.

6. Test results II: circumferential and volumetric behavior

Figure 12 shows the cyclic behavior of confined specimens in the circumferential direction versus stress in the axial direction. The SMA-wire-jacketed specimens showed larger areas of hysteretic loops than the steel-jacketed specimens. However, the area did not represent energy dissipation or damping in the circumferential direction because the stress was perpendicular to the strain.

6.1. Plastic and recovered strains in the circumferential direction

As in the axial direction, the plastic strain in the circumferential direction was investigated. Also, the recovered strain which is the amount of unloading strain minus the plastic strain was assessed. Both strains are shown in figure 13. The SMA wire and the steel jackets showed the same slopes regardless of the volumetric ratios of the jackets. However, the steel jackets showed steeper slopes than the SMA wire jackets; thus, there remained more plastic strain. The recovered strains increased at first and then became stable for the steel jackets. However, the SMA wire jackets increased the recovered strains continuously. The recovered strains for the SMA-wire-jacketed specimens for the stable plateau were approximately 2.5–3 times larger than those for the steel-jacketed specimens. In axial behavior, the plastic strains showed a similar behavior for the SMA wire and steel-jacketed specimens; therefore, the recovered strains were considered to be similar, too. However, in circumferential behavior, the SMA-wire-jacketed specimens recovered more circumferential strain. The cause of this was assumed to be active confinement and the elastic behavior of the SMA wire against the bulging of the concrete cylinders in the circumferential direction. In contrast to the SMA wire jackets, the steel jackets provided only passive confinement and showed plastic behavior.

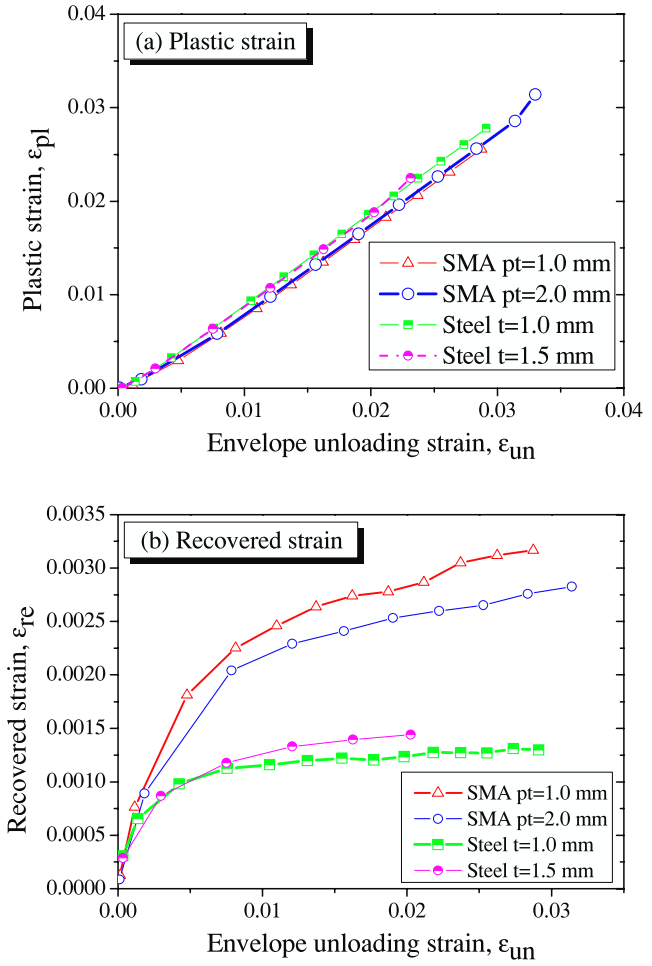

Figure 13. Plastic and recovered strain in circumferential direction. (a) Plastic strain. (b) Recovered strain.

6.2. Volumetric strains

Volumetric strain is calculated as

$$\varepsilon_{\text{vol}} = -\varepsilon_{\text{axial}} + 2\varepsilon_{\text{circum}} \tag{4}$$

where, $\varepsilon_{\text{axial}}$ and $\varepsilon_{\text{circum}}$ represent strains in the axial direction and the circumferential direction, respectively. In equation (4), positive strain indicates expansion of volume, and negative strain indicates contraction. Figure 14 shows the volumetric strains for the jacketed specimens versus axial stress. After the peak strength points, the steel-jacketed specimens slightly increased in volume during an unloading path; however, the SMA wire jackets restricted the increment of volume during an unloading path. The SMA wire jackets reduced the volume of the specimens during a reloading phase after the peak point. However, for the steel-jacketed specimens, the reloading paths nearly followed the unloading paths; thus, the steel jackets changed the volume very little during a reloading phase. The results showed that the SMA wire jackets more effectively restricted the expansion of concrete cylinder volume than the steel jackets after the peak strength point.

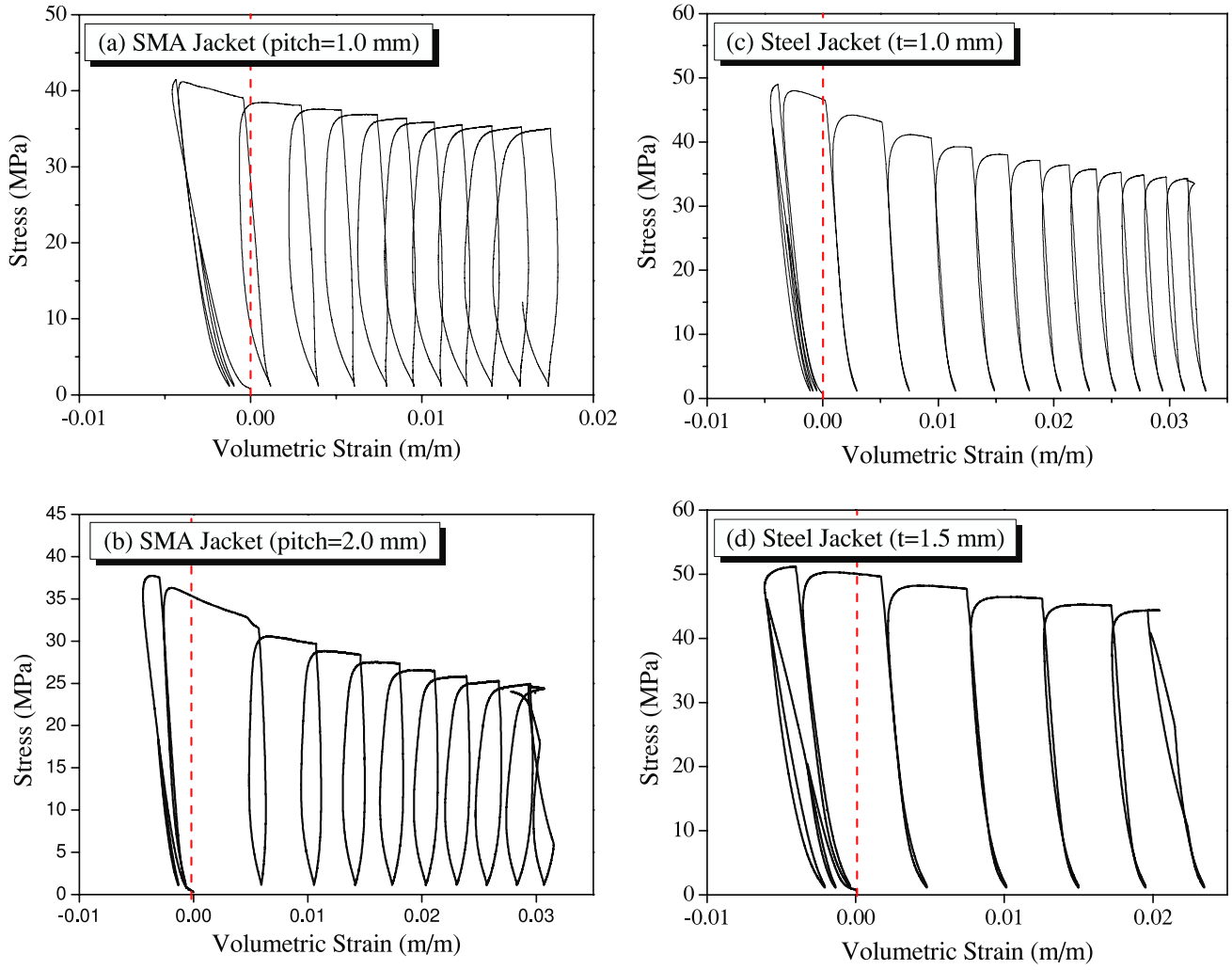

Figure 14. Volumetric strain for the jacketed specimens. (a) SMA jacket with 1.0 mm pitch. (b) SMA jacket with 1.0 mm pitch. (c) SMA jacket with 1.0 mm pitch. (d) SMA jacket with 1.0 mm pitch.

7. Test results III: SMA wire behavior during a cyclic test

The behavior of SMA wires and steel jackets in the circumferential direction was estimated in figure 15. The graphs were drawn manually based on the test data. The behavior of an SMA wire overlaps the behavior under residual stress in figure 15(a). The stress of the SMA wire was up and down due to cyclic loading but increased overall with increasing circumferential strain. The SMA wire showed a hysteretic loop in each cyclic loading; this behavior was considered to restrict the volume of expansion specimens. It appears that the loop behavior of the SMA wire produced the constriction of volume during the reloading path in figures 14(a) and (b) and increased the hysteretic damping effect. The steel jackets showed elastic–plastic behavior in the circumferential direction during a cyclic test, and the unloading and reloading paths were identical. The hardening effect of steel was ignored in figure 15(b). The steel jackets did not reduce the volume of specimens during reloading paths. The same path of unloading and reloading of steel after the yield seemed to induce the same path of unloading and reloading in volumetric strain curves in figures 14(c) and (d). Therefore, it was found that the different behavior of the volumetric strain curves in figure 14 was caused from the different behavior of the jacketing materials.

8. Conclusions

This study conducted cyclic tests on concrete confined by SMA wire and steel jackets. The SMA wire jackets provided active and passive confinement of concrete. The tensile behavior of the SMA wire under residual stress was tested to understand the SMA wire behavior due to cyclic loadings.

The residual stress that provided active confinement decreased with increasing applied strain and became zero when the applied strain reached the original prestrain. Beyond the prestrain, no residual strain or residual stress remained in the SMA wire. The reduction of the residual stress due to introduction additional strain was almost constant.

The cyclic behavior of SMA wire and steel-jacketed concrete was similar to the results obtained in previous

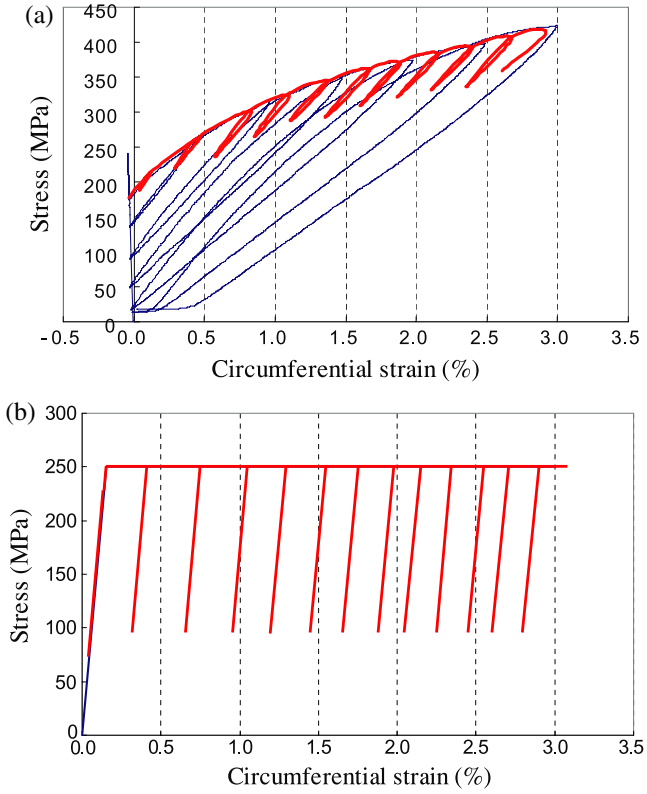

Figure 15. SMA wire and steel behavior during a cyclic loading test. (a) SMA wire behavior. (b) Steel jacket behavior.

studies. However, the envelopes of the hysteretic curve for the SMA wire jacket with 1.0 mm pitch differed from the monotonic behavior. This seemed to be due to the behavioral characteristics of the martensitic SMA. The plastic strains of the SMA wire and steel-jacketed concrete showed a similar trend. This study modified an existing plastic strain equation from a previous study, and the proposed equations predicted the experimental results almost perfectly. The modified equations for the SMA wire and the steel-jacketed concrete were similar to each other.

This study estimated the stress deterioration ratio for the confined concrete. The ratio for the steel-jacketed concrete showed a similar value to that of the previous study. Also, the ratios for the SMA-wire-jacketed concrete were a little larger than that of the steel-jacketed concrete; however, the difference was about 3%. Thus, it can be said that the cyclic behavior of the SMA-wire-jacketed concrete was similar to that of the steel-jacketed concrete.

The circumferential behavior of the SMA-wire-jacketed specimens differed from that of the steel-jacketed specimens. The SMA wire jackets recovered more circumferential strain than the steel jackets. For volumetric strain, the SMA wire jackets constricted the volume of specimens during a reloading path; however, the steel jackets did not show such behavior. Finally, this study showed the cyclic behavior of an SMA wire during a cyclic test. The SMA wire showed a hysteretic loop for each cyclic loading, and the stress of the wire increased overall with increasing circumferential strain. The used SMA wires were not trained. If the wires were trained against cyclic loadings, the results may be changed since trained SMA wires show more stable behavior. Therefore, a further study is required related to this topic.

Acknowledgments

This study has been supported by the Basic Science Research Program through the National Research Foundation of Korea funded by the Ministry of Education, Science, and Technology (project no. 2009-0087163).

References

[1] Saiidi M S and Wang H 2006 Exploratory study of seismic response of concrete columns with shape memory alloys reinforcement *ACI Struct. J.* **103** 436–43

[2] Saiidi M S, O'Brien O and Sadrossadat-Zadeh M 2009 Cyclic response of concrete bridge columns using superelastic nitinol and bendable concrete *ACI Struct. J.* **106** 69–77

[3] Choi E, Chung Y S, Choi J H, Kim H T and Lee H 2010 The confining effectiveness of NiTiNb and NiTi SMA wire jackets for concrete *Smart Mater. Struct.* **19** 035024

[4] Choi E, Cho S C, Hu J W, Park T and Chung Y S 2010 Recovery and residual stress of SMA wires and application for concrete structures *Smart Mater. Struct.* **19** 094013

[5] Andrawes B, Shin M and Wierschem N 2010 Active confinement of reinforced concrete bridge columns using shape memory alloys *J. Bridge Eng.* **15** 81–9

[6] Youssef M A, Alam M S and Nehdi M 2008 Experimental investigation on the seismic behavior of beam-column joints reinforced with superelastic shape memory alloys *J. Earthq. Eng.* **12** 1205–22

[7] Ocel J, DesRoches R, Leon R T, Hess W G, Krumme R, Hayes J R and Sweeney S 2004 Steel beam-column connections using shape memory alloys *J. Struct. Eng., ASCE* **130** 732–40

[8] Penar B W 2005 Recentering beam-column connections using shape memory alloys *Master's Thesis* Georgian Institute of Technology

[9] DesRoches R, Taftali B and Ellingwood B R 2010 Seismic performance assessment of steel frames with shape memory alloy connections, part I—analysis and seismic demands *J. Earthq. Eng.* **14** 471–86

[10] Hu J W, Choi E and Leon R T 2011 Design, analysis and application of innovative composite PR connections between steel beams and CFT columns *Smart Mater. Struct.* **20** 025019

[11] DesRoches R, McCormick J and Delemont M 2004 Cyclic properties of superelastic shape memory alloy wires and bars *J. Struct. Eng., ASCE* **130** 38–46

[12] DesRoches R and Delemont M 2002 Seismic retrofit of simply supported bridges using shape memory alloys *Eng. Struct.* **24** 325–32

[13] DesRoches R and Muthukumar S 2002 Effect of pounding and restrainers on seismic response of muliple-frame bridges *J. Struct. Eng., ASCE* **128** 860–9

[14] Andrawes B and DesRoches R 2007 Comparison between shape memory alloy seismic restrainers and other bridge retrofit devices *J. Bridge Eng., ASCE* **12** 700–9

[15] Choi E, Lee D H and Choei N Y 2009 Shape memory alloy bending bars as seismic restrainers for bridges in seismic areas *Int. J. Steel Struct.* **9** 261–73

[16] Choi E, Park J, Yoon S J, Choi D H and Park C 2010 Comparison of seismic performance of three restrainers for multiple-span bridges using fragility analysis *Nonlinear Dyn.* **61** 83–99

[17] Wilde K, Gardoni P and Fukino Y 2000 Base isolation system with shape memory alloy device for elevated highway bridge *Eng. Struct.* **22** 222–9
[18] Miyazaki S, Imai T, Igo Y and Otsuka K 1986 Effect of cyclic deformation on the pseudoelasticity characteristics of Ti–Ni alloys *Metall. Mater. Trans.* A **17** 115–20
[19] McCormick J, Barbero L and DesRoches R 2005 Effect of mechanical training on the properties of superelastic shape memory alloys for seismic applications *Smart Structures and Materials*; *Proc. SPIE* **5764** 430–9
[20] Kim S and Cho M 2010 A simple smart wing actuator using Ni–Ti SMA *J. Mech. Sci. Technol.* **24** 1865–73
[21] Choi E, Nam T H, Cho S C, Chung Y S and Park T 2008 The behavior of concrete cylinders confined by shape memory alloy wires *Smart Mater. Struct.* **17** 065032
[22] Choi E, Nam T H and Yoon S J 2009 A new steel jacketing method for RC columns *Mag. Concr. Res.* **61** 787–96
[23] Sakai J and Kawashima K 2006 Unloading and reloading stress–strain model for confined concrete *J. Struct. Eng., ASCE* **132** 112–22
[24] Bahn B H and Hsu C T 1998 Stress–strain behavior of concrete under cyclic loading *ACI Mater. J.* **95** 178–93
[25] Lam L and Teng J G 2009 Stress–strain model for FRP-confined concrete under cyclic axial compression *Eng. Struct.* **31** 308–321